(pumps), vasculature (tubes with resistive and capacitive function), and blood. These three components interactively determine all hemodynamic variables. Of these, pump function and resistive function of vasculature have been repeatedly evaluated in previous studies. These properties were also evaluated clinically.

In contrast, evaluation of the vascular capacitive function and that of the blood volume have been relatively ignored. Even though blood volume drastically changes, there have been no reasonable methods to evaluate total stressed blood volume precisely. Simple measurement of central venous pressure (i.e., RAP) cannot be a proxy marker of blood volume, as this pressure value also changes with pump function or with redistribution of blood.

It is clear from our results [$V = (CO + 19.61\ RAP + 3.49\ LAP) \times 0.129$] that blood volume (V) is not solely determined by RAP. Rather, all three variables CO, RAP and LAP contribute (not as differently as have been considered) to the changes in blood volume. Clinicians should know that when LAP increases by 5.6 mmHg, or CO increases by 0.98L/min in 50-Kg patients, similar blood volume increases as RAP is increased by 1 mmHg.

Implantable devices with volume monitoring functionality for patients with heart failure should also take these results into consideration.

B. Hemodynamic Variables and Cardiovascular Properties

In clinical practice, physicians have to restore hemodynamic variables to their respective normal range. Of these, the most important three variables include blood pressure, CO and LAP. These variables are essentially important as blood pressure determines the perfusion of vital organs (for short-term need), CO determines the perfusion of peripheral tissues (for long-term need), and LAP determines blood oxygenation in lungs.

These hemodynamic variables are, in turn, determined by the interaction between cardiovascular properties, such as pump, resistance, capacitance, and blood volume. What clinicians should know, monitor, and correct are in reality these cardiovascular properties. Most drugs and interventions are aimed at correcting mainly one of these properties. From these viewpoints, the method to continuously estimate cardiovascular properties from measured hemodynamics is the most basic need in patient monitoring.

V. Conclusion

We have successfully developed a method to estimate the cardiac output curve and venous return surface from a single hemodynamic data set. This method enabled to predict new hemodynamics after withdrawal or transfusion of blood of known volume.

References

[1] A. C. Guyton, "Determination of cardiac output by equating venous return curves with cardiac response curves," *Physiol. Rev.* vol. 35, no. 1,123–129, Jan. 1955.

[2] K. Uemura, M. Sugimachi, T. Kawada, A. Kamiya, Y. Jin, *et al.*, "A novel framework of circulatory equilibrium," *Am. J. Physiol. Heart Circ. Physiol.* vol. 286, no. 6, pp. H2376–H2385, Jun. 2004.

[3] K. Uemura, T. Kawada, A. Kamiya, T. Aiba, I. Hidaka, *et al.*, "Prediction of circulatory equilibrium in response to changes in stressed blood volume," *Am. J. Physiol. Heart Circ. Physiol.* vol. 289, no. 1, H301–H307, Jul. 2005.

32nd Annual International Conference of the IEEE EMBS
Buenos Aires, Argentina, August 31 - September 4, 2010

How to quantitatively synthesize dynamic changes in arterial pressure from baroreflexly modulated ventricular and arterial properties

Takafumi Sakamoto, Yoshinori Murayama, Tomoyuki Tobushi, Kazuo Sakamoto, Atsushi Tanaka, Takaki Tsutsumi, and Kenji Sunagawa, Senior *Member, IEEE*

Abstract—**Baroreflex regulates arterial pressure by modulating ventricular and vascular properties. We investigated if the framework of circulatory equilibrium that we developed previously (Am J Physiol 2004, 2005) by extending the classic Guyton's framework is capable of predicting baroreflex induced changes in arterial pressure. In animal experiments, we estimated open loop transfer functions of baroreflexly modulated ventricular and vascular properties, synthesized baroreflex induced dynamic changes in arterial pressure using the estimated transfer functions and compared the predicted responses with measured responses. We demonstrated that the predicted baroreflex induced changes in arterial pressure matched reasonable well with those measured. We conclude that the framework of circulatory equilibrium is generalizable under the condition where baroreflex dynamically changes arterial pressure.**

I. Introduction

Baroreflex is known to be the fastest mechanism in the body to stabilize arterial pressure (AP). This AP stabilization is achieved by feedback regulation of ventricular and vascular properties [1-3]. However, how those changes in mechanical properties quantitatively impact AP remains unknown. We previously developed a framework of circulatory equilibrium where we introduced the left atrial pressure-cardiac output (CO) relationship into the classic Guyton's framework and expanded the venous return (VR) curve to the VR surface. We then expressed the CO curves and VR surface using end-systolic elastance (Ees), heart rate (HR), vascular resistance (R) and stressed blood volume (V) [4, 5] and derived the circulatory equilibrium as the intersection between the CO curve and VR surface. The purpose of this investigation is if the extended Guyton's framework can quantitatively predict dynamic AP responses by incorporating the baroreflexly modulated ventricular and arterial properties.

Manuscript received April 23, 2010. This work was supported in part by Health and Labour Sciences Research Grant for Research on Medical Devices for Improving Impaired QOL from the Ministry of Health Labour and Welfare of Japan, Health and Lobour Sciences Research Grant for Clinical Research from the Ministry of Health Labour and Welfare of Japan, and Grant-in-Aid for Scientific Research(S) (18100006) from the Japan Society for the Promotion of Science

T. Sakamoto, Y. Murayama, T. Tobushi, K. Sakamoto, A. Tanaka and K. Sunagawa are with Kyushu university, Fukuoka 8128582 Japan. (corresponding author Takafumi Sakamoto to provide phone: +81-92-642-5360; fax: +81-92-642-5357; e-mail: tsaka@cardiol.med.kyushu-u.ac.jp).

T. Tsutsumi is with Iizuka Hospital, Iizuka 8208505 Japan (e-mail: tsutsumi@cardiol.med.kyushu-u.ac.jp).

II. Methods

A. A framework of circulatory equilibrium

The framework of circulatory equilibrium consists of the VR surface representing VR of the systemic and pulmonary circulations and the integrated CO curve representing the pumping ability of the left (LV) and right ventricle (RV) (Fig. 1) [4, 5]. The integrated CO curve and VR surface (CO*v*) are formulated as

$$CO = \frac{1}{k} \times \frac{Ees}{Ees/HR + R} \times \{\log(Pat - F) + H\}$$

and

$$COv = V/w - Gp \times P_{LA} - Gs \times P_{RA}$$

respectively, where Pat is left atrial pressure (P_{LA}) for LV and right atrial pressure (P_{RA}) for RV. k, F, H, w, Gp and Gs are empirically derived constants. Once we obtain a set of Ees, R, HR and V, we derive CO by the framework and estimate AP by multiplying CO and R [4, 5].

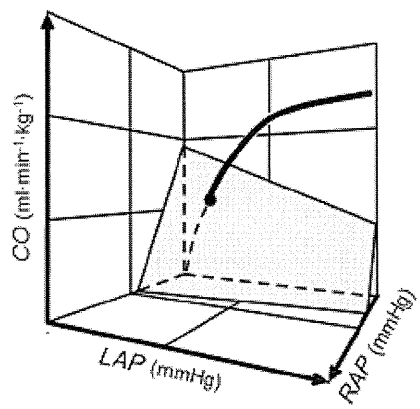

FIG.1 A FRAMEWORK OF CIRCULATORY EQUILIBRIUM

B. Animal preparation

Animal care was in accordance with institutional guidelines. Six mongrel dogs weighing 16.5±1.2kg (mean±SD) were anesthetized with pentobarbital sodium. We cut the vagosympathetic trunk to eliminate other reflexes and isolated

the bilateral carotid sinuses from the systemic circulation and connected them to a servo pump to control intrasinus pressure (CSP). An ultrasonic flow probe was placed around the ascending aorta to measure CO. We implanted two pairs of sonomicrometer in the epicardium and inserted a micromanometer into LV via the apex to measure Ees. We measured AP, P_{LA} and P_{RA}. Stressed blood volume was estimated from the VR surface. All analog data were digitalized at 200Hz with 12-bit resolution.

C. *Identification of the transfer function*

We perturbed CSP with pseudorandom binary sequences (100 and 180 mmHg) with a shortest interval of 5 seconds to identify the open-loop transfer functions from CSP to Ees, HR, R and V. We estimated the transfer functions in the frequency range between 0.002 to 0.1 Hz. To quantify the linear dependence between the input and output signals in the frequency domain, we also estimated a magnitude-squared coherence function.

D. *Prediction of the dynamic change of AP*

To validate the framework of circulatory equilibrium, we predicted Ees, HR, R and V using those estimated transfer functions in response to changes in CSP in data sets that had not been used to estimate the transfer functions. We then predicted APs using the developed framework and compared them against measured.

III. RESULTS

Mean AP, HR, Ees, R and V during perturbations were 124±22 mmHg, 168±13 bpm, 11.3±2.9 mmHg/ml, 1.37±0.27 ml/(ml/min/kg) and 18.8±3.7 ml/kg, respectively. These values are comparable to those previously reported [4, 5].

Shown in Fig. 2 is the transfer function from CSP to Ees in an animal. The transfer function approximates a second-order delay system with a cut-off frequency of 0.023 Hz. These finding are consistent with that reported [2].

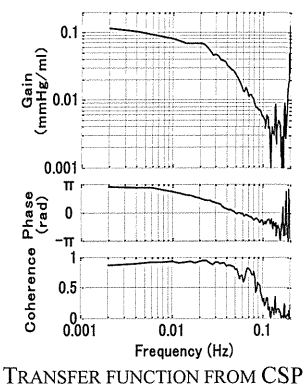

FIG. 2. TRANSFER FUNCTION FROM CSP TO Ees

Illustrated in Fig. 3 are the time series of CSP, predicted AP (solid line) and measured AP (dotted line) in an animal. The predicted AP matches reasonably well with those measred. The correlation coefficent (r2) varied between 0.80 and 0.93. The standard error of estimate ranged between 4.4 and 7.6 mmHg (3.0-7.2 % of mean AP) suggseting the reasonable accuracy of prediction.

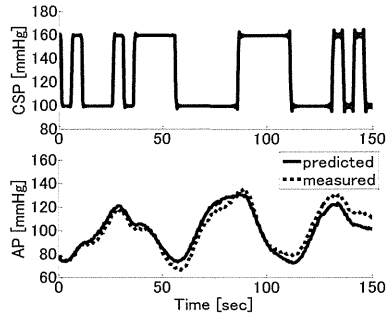

FIG. 3. PREDICTION OF THE DYNAMIC CHANGE OF AP

IV. DISCUSSION

We have shown that the framework of circulatory equilibrium, which is an extension of the classic Guyton's framework, could predict the changes of AP induced by baroreflexly modulated ventricular and vascular properties.

The extended Guyton's framework developed by the authors' group has been shown to accurately represent the circulatory equilibrium under steady state conditions [4, 5]. However, whether the model holds under dynamic conditions remained unanswered. Furthermore, in the present study, we predicted the dynamic baroreflex induced responses of Ees, HR, R and V with a set of linear transfer functions. Since the baroreflex system is known to be nonlinear, how the nonlinearity in the baroreflex system impacts the accuracy of predictions remained unknown. The results of present study indicated that we could linearly predict baroreflexly modulated ventricular and vascular properties reasonably well and the framework of circulatory equilibrium holds under the condition where baroreflex dynamically changes arterial pressure.

V. CONCLUSION

We conclude that the proposed framework of circulatory equilibrium holds under baroreflex induced dynamic changes in hemodynamic conditions.

ACKNOWLEDGMENT

This study was supported in part by Health and Labour Sciences Research Grant for Research on Medical Devices for Improving Impaired QOL from the Ministry of Health Labour and Welfare of Japan, Health and Labour Sciences Research Grant for Clinical Research from the Ministry of Health Labour and Welfare of Japan, and Grant-in-Aid for Scientific Research(S) (18100006) from the Japan Society for the Promotion of Science.

REFERENCES

[1] A.C. Guyton, and John E. Hall, "Textbook of Medical Physiology, eleventh edition", *pp. 230-231. 2006.*

[2] T. Kubota, J. A. Alexander Jr, R. Itaya, K. Todaka, M. Sugimachi, K. Sunagawa, Y. Nose and A. Takeshita, "Dynamic effects of carotid

sinus baroreflex on ventriculoarterial coupling studied in anesthetized dogs,'' *Circulation Research ; 70: 1044-1053, 1992.*

[3] A. A. Shoukas, ''Carotid sinus baroreceptor reflex control and epinephrine. Influence on capacitive and resistive properties of the total pulmonary vascular bed of the dog,'' *Circulation Research ; 51; 95-101, 1982*

[4] K. Uemura, M. Sugimachi, T. Kawada, A. Kamiya, Y. Jin, K. Kashihara, and K. Sunagawa, "A novel framework of circulatory equilibrium,'' *Am J Physiol Heart Circ Physiol 286: H2376-H2385, 2004.*

[5] K. Uemura, T. Kawada, A. Kamiya, T. Aiba, I. Hidaka, K. Sunagawa, and M. Sugimachi, "Prediction of circulatory equilibrium in response to changes in stressed blood volume,'' *Am J Physiol Heart Circ Physiol 289: H301-H307, 2005.*

Atherosclerosis 213 (2010) 52–58

Contents lists available at ScienceDirect

Atherosclerosis

journal homepage: www.elsevier.com/locate/atherosclerosis

Acetylcholinesterase inhibitors attenuate atherogenesis in apolipoprotein E-knockout mice

Keita Inanaga[a], Toshihiro Ichiki[a,b,*], Ryohei Miyazaki[a], Kotaro Takeda[a,b], Toru Hashimoto[a], Hirohide Matsuura[a], Kenji Sunagawa[a]

[a] Department of Cardiovascular Medicine, Kyushu University Graduate School of Medical Sciences, Japan
[b] Department of Advanced Therapeutics for Cardiovascular Diseases, Kyushu University Graduate School of Medical Sciences, Japan

ARTICLE INFO

Article history:
Received 16 February 2010
Received in revised form 7 July 2010
Accepted 18 July 2010
Available online 27 July 2010

Keywords:
Cholinesterase inhibitor
Donepezil
Apolipoprotein E-knockout mice
Oxidative stress
Cytokine

ABSTRACT

Objective: Donepezil, a reversible acetylcholinesterase inhibitor, improves cognitive function of Alzheimer's disease. Stimulation of cholinergic system was reported to improve long-term survival of rats with chronic heart failure and to attenuate inflammatory response in mice with lipopolysaccharide-induced sepsis. We sought to determine whether the pharmacological stimulation of cholinergic system by donepezil reduces atherogenesis in apolipoprotein (Apo) E-knockout (KO) mice.

Methods and results: Male ApoE-KO mice (10-week-old) were fed a high-fat diet and received infusion of angiotensin (Ang) II (490 ng/kg/day). Donepezil or physostigmine was administered for 4 weeks. Oral administration of donepezil (5 mg/kg/day) or infusion of physostigmine (2 mg/kg/day) significantly attenuated atherogenesis (Oil Red O-positive area) without significant changes in heart rate, blood pressure and total cholesterol levels. Administration of donepezil suppressed expression of monocyte chemoattractant protein-1 and tumor necrosis factor-α, NADPH oxidase activity and production of reactive oxygen species in the aorta.

Conclusion: The present study revealed novel anti-oxidative and anti-atherosclerotic effects of pharmacological stimulation of cholinergic system by donepezil. Donepezil may be used as a novel therapeutics for the atherosclerotic cardiovascular diseases.

1. Introduction

Activation of vagus nerve shows various effects on hemodynamics. It slows heart rate, dilates blood vessel and reduces blood pressure. Results of the Autonomic Tone and Reflexes After Myocardial Infarction Study and the Cardiac Insufficiency Bisoprolol Study II indicate that diminished cardiac vagus activity predicts the higher mortality rate in patients with chronic heart failure [1,2]. In addition, vagus nerve stimulation (VNS) improves long-term survival of rats with chronic heart failure after experimental myocardial infarction [3]. VNS modulates the cardiac redox status and adrenergic drive, and thereby suppresses free radical generation in the failing heart [4]. However, the effect of VNS on vascular lesion formation has not been reported.

Stimulation of cholinergic system was reported to attenuate tumor necrosis factor (TNF)-α production from macrophages and hypotensive shock in a lipopolysaccharide (LPS)-induced septic model [5,6]. Stimulation of cholinergic system inhibits activation of nuclear factor-kappa B (NF-κB) [7] and induces suppressor of cytokine signal 3 expression [8], resulting in the attenuation of inflammatory responses. However, nicotine, a nicotinic acetylcholine receptor (AchR) agonist, was reported to induce endothelial dysfunction that is an initial step of atherosclerosis and to accelerate atherosclerosis in Apolipoprotein E-knockout (ApoE-KO) mice [9]. Therefore, it is not clear whether the activation of cholinergic system is atherogenic or atheroprotective.

Donepezil [diethyl(3,5-di-ter-butyl-4-hydroxybenzyl)phosphonate] is a long acting, reversible cholinesterase inhibitor and is known to improve memory and cognitive function in patients with Alzheimer's disease [10]. A recent study showed that treatment of patients with Alzheimer's disease with donepezil for 1 month reduces production of oncostatin-M, interleukin (IL)-6 and IL-1 in the peripheral blood mononuclear cells [11], suggesting a possible anti-inflammatory effect of donepezil. However, the mechanism remains to be determined.

Angiotensin (Ang) II plays critical roles in the progression of atherosclerosis, ventricular remodeling after myocardial infarction and heart failure [12]. One of the mechanisms by which AngII

* Corresponding author at: Department of Cardiovascular Medicine, Kyushu University Graduate School of Medical Sciences, 3-1-1 Maidashi, Higashiku, 812-8582 Fukuoka, Japan. Tel.: +81 92 642 5361; fax: +81 92 642 5374.
E-mail address: ichiki@cardiol.med.kyushu-u.ac.jp (T. Ichiki).

0021-9150/$ – see front matter © 2010 Elsevier Ireland Ltd. All rights reserved.
doi:10.1016/j.atherosclerosis.2010.07.027

accelerates atherogenesis is the induction of oxidative stress and inflammation [13]. AngII activates NADPH oxidase in the blood vessel resulting in the activation of redox-sensitive transcription factors such as nuclear factor (NF)-B and activating protein (AP)-1 [14], resulting in the production of inflammatory cytokines or chemokines such as TNF-α, IL-6, and monocyte chemoattractant protein (MCP)-1.

These previous studies prompted us to examine the effect of pharmacological stimulation of cholinergic system by donepezil on the progression of atherosclerosis in ApoE-KO mice. In the present study we showed that donepezil attenuated atherogenesis in ApoE-KO mice fed a high-fat diet (HFD) with or without AngII stimulation, possibly through anti-oxidative and anti-inflammatory effects.

2. Materials and methods

2.1. Materials

AngII was purchased from PEPTIDE Institute Inc. Physostigmine, Ach, lucigenin, β-nicotinamide adenine dinucleotide 2′-phosphate reduced hydrate (NADPH) were purchased from Sigma Chemical Co. Donepezil was purchased from Toronto Research Chemicals Inc. Antibodies against p47phox and NOX1 were purchased from Santa Cruz Biotechnology, Inc. Other chemical reagents were purchased from Wako Pure Chemicals, unless mentioned specifically.

2.2. Animal model of atherosclerosis

All procedures were approved by the committee on Ethics of Animal Experiment, Kyushu University Graduate School of Medical Sciences and conducted in accordance with the Guide for the Care and Use of Laboratory Animals published by the US National Institutes of Health.

C57BL/6J ApoE-KO mice were purchased from the Jackson Laboratory. Male ApoE-KO (10-week-old) mice were fed a HFD (35% calorie from fat, 1% cholesterol) and received infusion of AngII (490 ng/kg/day) through an osmotic minipump (Alzet) implanted in the peritoneal cavity for 4 weeks. Mice had an ad libitum access to both food and water. Four groups were compared: control, AngII + HFD, AngII + HFD and donepezil (estimated dose of ingestion: 5 mg/kg/day via drinking water), and AngII + HFD and physostigmine (2 mg/kg/day via second osmotic minipump). Blood pressure and heart rate were monitored using a computed tail-cuff system (UR-5000, UEDA, Ueda Co. Ltd.). The doses of cholinesterase inhibitors were chosen on the basis of previous studies that showed that donepezil [15] or physostigmine [16] at the doses mentioned above did not affect heart rate or blood pressure level in mice.

In another experiment, ApoE-KO mice (12-week-old) were fed a HFD only for 8 weeks without AngII. And the effect of donepezil was examined.

2.3. Histological and immunohistochemical analyses

At the end of experiments, mice were anesthetized with an intraperitoneal injection of pentobarbital. The circulatory system was perfused with PBS via the left ventricle. Then, the aortic arch and the thoracic aorta was opened longitudinally, stained with Oil Red O, and pinned out on a black wax surface. The percentage of the plaque area stained by Oil Red O to the total luminal surface area was determined. Serial sections of the aortic root were prepared and were stained with the antibodies against macrophage (F4/80; Serotec Inc.) and MCP-1 (Santa Cruz Biotechnology Inc.). All images were captured with a Nikon microscope equipped with a video camera and analyzed using Adobe Photoshop and Scion Image Software.

2.4. Tissue preparation

The thoracic and abdominal aorta were immediately frozen in liquid nitrogen for RNA isolation, Lucigenin assay, and Western blot analysis. For RNA isolation, thoracic aorta was additionally perfused with RNA Later (Ambion) to prevent RNA degradation. Frozen samples of thoracic aorta were crashed on dry ice and homogenized in ISOGEN (Nippon Gene) and total RNA was prepared in accordance with the manufacturer's instruction.

2.5. Real-time reverse transcription polymerase chain reaction analysis

Reverse transcription of RNA was performed with ReverTra Ace (TOYOBO). Quantitative real-time reverse transcription polymerase chain reaction (qRT-PCR) was performed using SYBR Green and the ABI PRISM 7500 Sequence Detection System (Applied Biosystems). The sequences of PCR primers used in this study are summarized in Supplemental Table 1. Primers for GAPDH were purchased from ABI, of which sequences are not disclosed.

2.6. Lucigenin-enhanced chemiluminescence assay

NADPH-dependent superoxide production was measured by lucigenin luminescence [17]. The aorta was perfused with ice cold PBS, immediately frozen in liquid nitrogen and the assay was performed on the same day. The frozen samples of abdominal aorta were crashed on dry ice and homogenized in modified Krebs buffer (99 mmol/L NaCl, 4.7 mmol/L KCl, 1.9 mmol/L $CaCl_2$, 1.2 mmol/L $MgSO_4$, 1.0 mmol/L K_2HPO_4, 25 mmol/L $NaHCO_3$, 20 mmol/L Na-HEPES, 11 mmol/L D-glucose). A luminescence assay was performed in a balanced salt solution (137 mmol/L NaCl, 2.7 mmol/L KCl, 4.3 mmol/L Na_2HpO_4, 1.5 mmol/L KH_2PO_4) buffer containing 5 μmol/L of lucigenin using a luminescence reader (Berthold Technology). The reaction was started by adding 100 μmol/L of β-NADPH as a substrate.

2.7. Oxidative fluorescent microphotography

Superoxide was detected in the layers of the vessel wall using fluorescent probe dihydroethidium (DHE; Molecular Probes) as described previously [18]. After perfusion with ice cold PBS, the ascending thoracic aorta was immediately frozen in OCT compound (Sakura Finetek) and stored at −80 °C until preparation for the cryosection. Cryosections (10 μm) were prepared in the next day and incubated for 30 min at 37 °C with 2 μmol/L DHE. Images were obtained on a confocal microscope (excitation filter at 488 nm; emission filter at 550 nm).

2.8. Western blot analysis

The aorta was homogenized in modified Krebs buffer. Protein concentrations were determined with the bicinchoninic acid protein assay kit (Pierce Chemical Co). The homogenates were heated in a sample buffer at 95 °C for 3 min, electrophoresed on 12% SDS-polyacrylamide gel, and transferred to polyvinylidene difluoride membrane (Immobilon-P, Millipore). Western blot analysis of p47phox, NOX1 and α-tubulin was performed by a conventional method and detected by ECL chemiluminescence (Amersham Pharmacia Biotech) according to the manufacturer's instructions. Membranes were scanned using LAS-4000mini bioimage analyzer (Fujifilm).

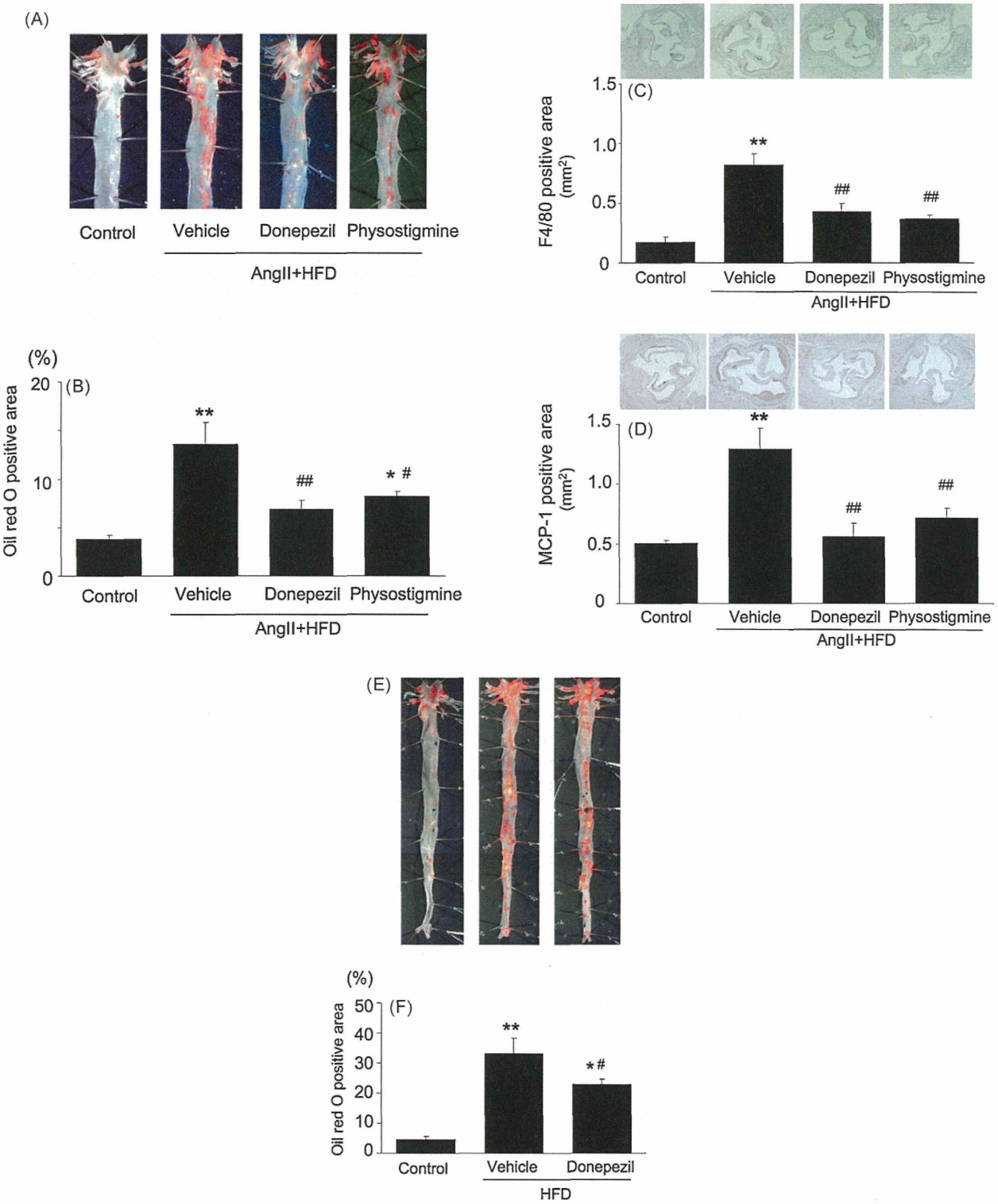

Fig. 1. Cholinesterase inhibitors attenuated atherogenesis in ApoE-KO mice. The effects of donepezil and physostigmine were examined in ApoE-KO mice fed a HFD and received AngII-infusion for 4 weeks (A–D). $n = 6$–8 (A) Oil Red O staining of the en face aorta is shown. (B) Bar graph indicates the percentage of Oil Red O-positive area in the aorta. (C) Immunohistochemical staining for macrophage by F4/80 antibody in the aortic cusp. Bar graph indicates F4/80-positive area. (D) Immunohistochemical staining for MCP-1 in the aortic cusp. Bar graph indicates MCP-1-positive area. Data are expressed as mean ± S.E.M. $^{*}P < 0.05$, $^{**}P < 0.01$ vs control, $^{\#}P < 0.05$, $^{\#\#}P < 0.05$ vs vehicle. The effect of donepezil was examined in ApoE-KO mice fed a HFD for 8 weeks (E and F). (E) Oil Red O staining of the en face aorta is shown. (F) Bar graph indicates the percentage of Oil Red O-positive area in the aorta. Data are expressed as mean ± S.E.M. $^{**}P < 0.01$ vs control, $^{\#}P < 0.05$ vs vehicle. Control $n = 5$, HFD or HFD + donepezil $n = 8$.

Table 1
HR, BP BW and total cholesterol levels in AngII + HFD groups.

	HR (bpm)	BP (mm Hg)	BW (g)	TC (mg/dl)
Control	610 ± 20	104 ± 2	28.8 ± 0.6	407 ± 21
AII + HFD	648 ± 17	124 ± 4**	27.2 ± 0.4	1981 ± 165**
AII + HFD + donepezil	618 ± 22	115 ± 4*	27.7 ± 1.0	1896 ± 63**
AII + HFD + physostigmine	657 ± 8	124 ± 3**	27.9 ± 0.7	2250 ± 70**

HR: heart rate, BP: blood pressure, BW: body weight, TC: total cholesterol.
* $P < 0.05$ vs control.
** $P < 0.01$ vs control.

2.9. Statistical analysis

Statistical analysis was performed with one-way ANOVA and Fisher's test, if appropriate. Data are shown as mean ± S.E.M. $P < 0.05$ was considered to be statistically significant.

3. Results

3.1. Cholinesterase inhibitors attenuated progression of atherosclerosis

To examine whether donepezil has anti-inflammatory and anti-atherosclerotic effects, we used HFD-fed ApoE-KO mice with AngII that accelerates vascular inflammation and thereby atherogenesis [13]. A combination treatment with AngII and HFD significantly increased blood pressure compared with control group. However, no significant differences in the heart rate, blood pressure and serum total cholesterol level were observed between AngII and HFD groups (Table 1). Body weight was slightly decreased in mice that received AngII and HFD compared with the control group. Oil Red O-positive area of en face aorta was reduced in mice treated with donepezil (Fig. 1A and B). Physostigmine, another cholinesterase inhibitor structurally unrelated to donepezil, also reduced Oil Red O-positive area, suggesting that inhibition of cholinesterase and a resultant increase in Ach availability are responsible for the attenuation of atherogenesis (Fig. 1A and B). Infiltration of macrophage (F4/80 antibody-positive cells) into the aortic root was also reduced in mice treated with donepezil or physostigmine (Fig. 1C). These cells expressed MCP-1 (Fig. 1D) and MCP-1-positive area was diminished by treatment with either donepezil or physostigmine, suggesting that cholinesterase inhibitors may attenuate atherogenesis through suppression of MCP-1 expression and macrophage recruitment.

We also examined the effect of donepezil on ApoE-KO mice fed a HFD for 8 weeks (from 12- to 20-week-old) without AngII-infusion. The Oil Red O-positive area was significantly suppressed by treatment with donepezil (Fig. 1E and 1F) without effects on hemodynamics and cholesterol level (Table 2).

3.2. Donepezil attenuated vascular reactive oxygen species (ROS) production and NADPH oxidase activity

ROS play an important role in atherogenesis. We, therefore, examined the effect of donepezil on ROS production. DHE staining showed that vascular ROS production was increased in ApoE-KO mice treated with AngII and HFD and that donepezil reduced the ROS production in the media (Fig. 2A). Lucigenin assay also showed that donepezil significantly reduced NADPH oxidase activity that is increased in AngII- and HFD-treated ApoE-KO mice (Fig. 2B). However, we did not see any effect of donepezil on the serum level of thiobarbituric acid reactive substance (data not shown), suggesting that donepezil might locally suppress oxidative stress in the aorta.

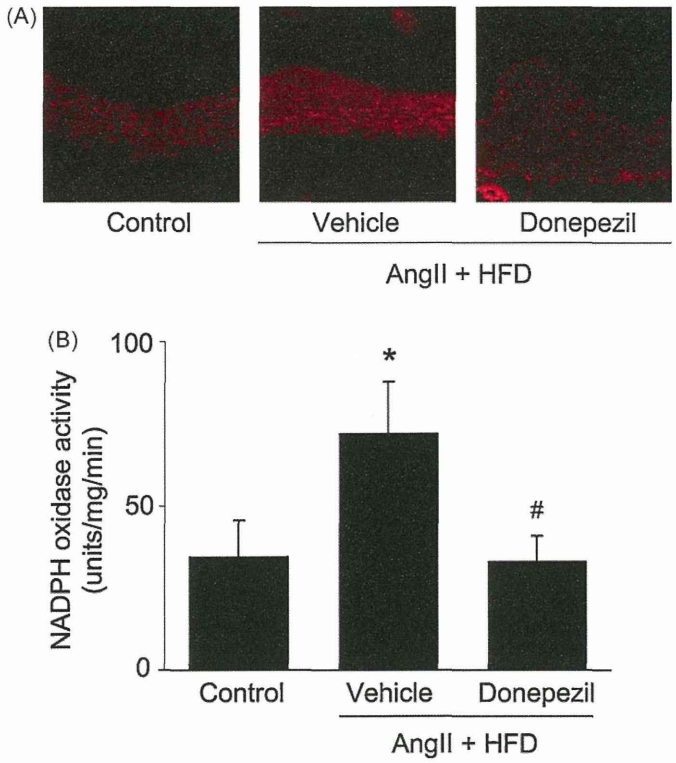

Fig. 2. The effect of donepezil on the oxidative stress in the aorta of ApoE-KO mice. (A) DHE staining revealed an increase in superoxide production in the aorta of AngII- and HFD-treated ApoE-KO mice. Donepezil reduced the extent of DHE staining. The same results were obtained in other 5 independent experiments. (B) Lucigenin assay showed that NADPH oxidase activity was increased by treatment with AngII and HFD in the aorta of ApoE-KO mice. Donepezil reduced the NADPH oxidase activity. Data are expressed as mean ± S.E.M. *$P < 0.05$ vs control, #$P < 0.05$ vs vehicle. $n = 6–8$.

Table 2
HR, BP BW and total cholesterol levels in HFD groups.

	HR (bpm)	BP (mm Hg)	BW (g)	TC (mg/dl)
Control	537 ± 13	99 ± 1	30.8 ± 0.6	555 ± 28
HFD	579 ± 15	97 ± 5	27.5 ± 0.7*	2173 ± 200**
HFD + donepezil	539 ± 19	100 ± 4	28.6 ± 1.2	2001 ± 96**

HR: heart rate, BP: blood pressure, BW: body weight, TC: total cholesterol.
* $P < 0.05$ vs control.
** $P < 0.01$ vs control.

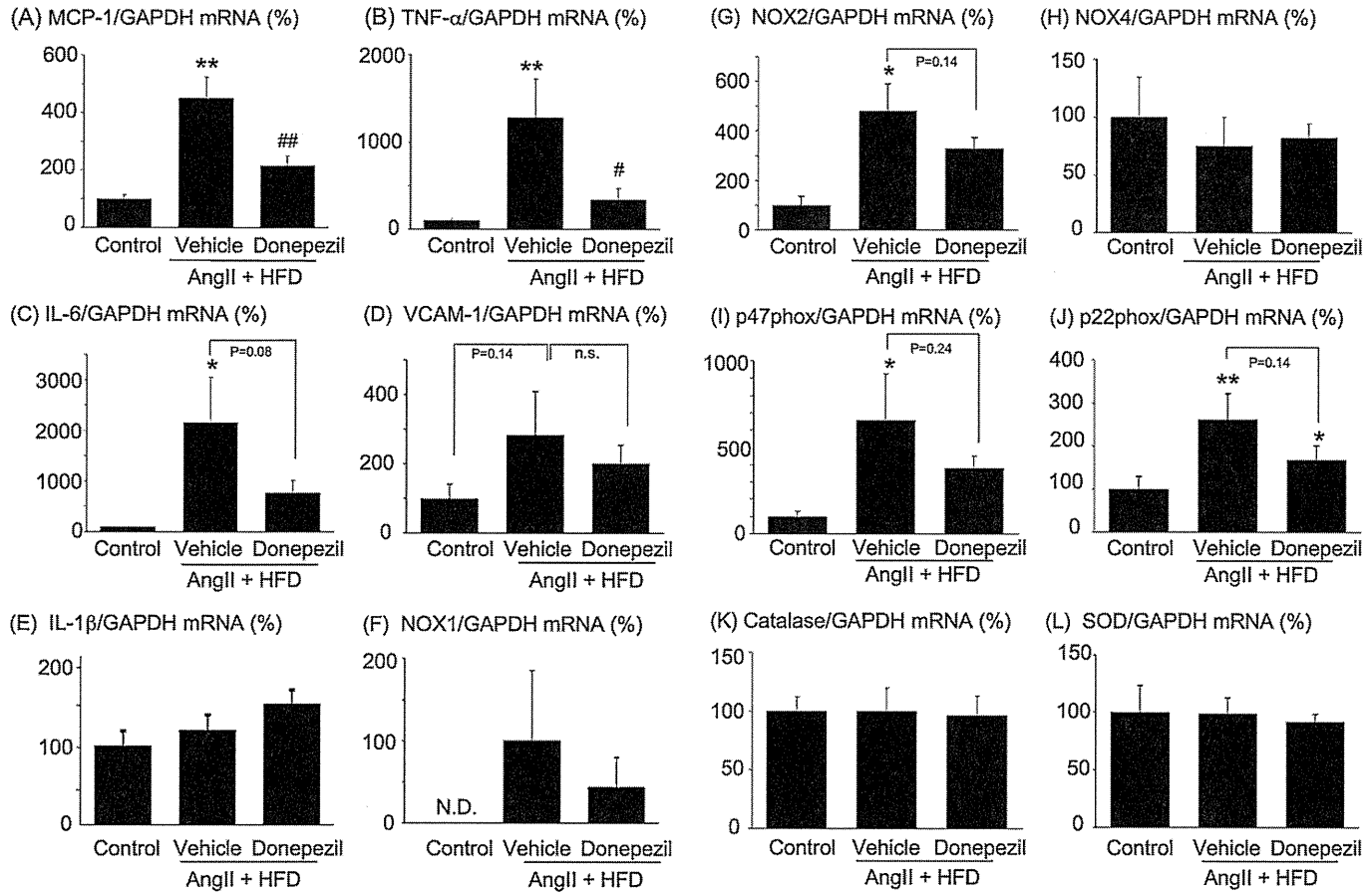

Fig. 3. Quantitative RT-PCR analyses for the mRNA expression in the aorta. mRNA expression of the aorta from control, AngII- and HFD- and AngII-, HFD- and donepezil-treated ApoE-KO mice was quantified with real-time RT-PCR. The primer sequences used were indicated in Supplemental Table 1. Data are expressed as mean ± S.E.M. $^{*}P<0.05$, $^{**}P<0.01$ vs control, $^{\#}P<0.05$, $^{\#\#}P<0.01$ vs vehicle. $n=7$–8. ND; not detected.

3.3. Donepezil attenuated MCP-1 and TNF-α mRNA expression

To gain insights into the molecular mechanism of anti-atherogenic effect of donepezil, mRNA expression of the aorta was examined by RT-PCR (Fig. 3). The combination treatment with AngII and HFD significantly increased MCP-1 and TNF-α mRNA expression in the aorta of ApoE-KO mice. Donepezil significantly attenuated both MCP-1 and TNF-α mRNA expression.

NOX1 is a major NADPH oxidase subunit expressed in VSMC [19]. Expression of NOX1 was slightly increased by AngII and a HFD, which was downregulated by donepezil. However, expression level of NOX1 is very low and the difference was not statistically significant.

Expression of other NADPH oxidase subunits (NOX2, p22phox, p47phox) was significantly increased in AngII and HFD group and donepezil attenuated the mRNA expression of these molecules. However, the reduction was not statistically significant. mRNA expression of NOX4, one of the NADPH oxidase subunit, superoxide dismutase, and catalase was not affected by the combination treatment with AngII and a HFD.

3.4. Donepezil inhibited p47phox and NOX1 protein level in the aorta

We examined protein expression of p47phox and NOX1 in the aorta. Western blot analysis revealed that expression level of p47phox was increased in ApoE-KO mice treated with HFD and AngII and the induction was significantly suppressed by donepezil (Fig. 4). The protein level of NOX1 was not affected among the three groups.

4. Discussion

We showed in the present study that donepezil and physostigmine attenuated progression of AngII accelerated atherosclerosis in ApoE-KO mice fed a HFD. The anti-atherogenic effect of donepezil was also observed in ApoE-KO mice fed a HFD without AngII-infusion. Donepezil attenuated NADPH oxidase activity and ROS production as well as cytokine expression in the aorta. These results suggest that cholinesterase inhibitor may be a novel strategy for the treatment of atherosclerotic cardiovascular diseases.

We chose ApoE-KO mice treated with HFD and AngII as an atherosclerotic model because AngII is known to induce inflammation and our hypothesis is that donepezil has an anti-inflammatory effect. It is of note that donepezil was more effective in HFD and AngII-infusion group than HFD group. Therefore, donepezil may be more effective against AngII-induced atherogenesis.

Custodis et al. showed that heart rate reduction by ivabradine, an inhibitor of I_f current in the sinoatrial node, attenuated atherogenesis in ApoE-KO mice [20]. In the present study, neither donepezil nor physostigmine significantly decreased heart rate, excluding the possible suppressive effect of bradycardia on atherogenesis. However, the reason why heart rate was not decreased by these cholinesterase inhibitors in our mice is not clear.

A recent meta-analysis by Singh et al. revealed that inhalation of anticholinergics is associated with a significantly increased risk of myocardial infarction and cardiovascular death but not with a risk of stroke in patients with chronic obstructive pulmonary disease (COPD) [21]. The results of the meta-analysis may support the idea that cholinergic system is atheroprotective. However, a very recent

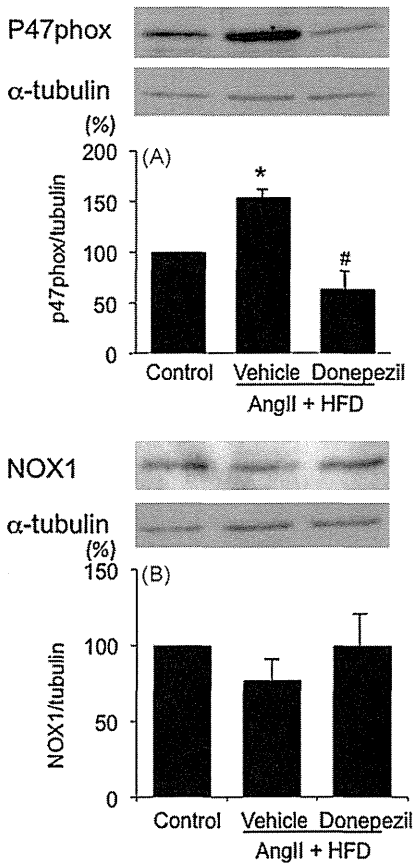

Fig. 4. Expression of p47phox and NOX1 protein in the aorta. Expression of p47phox and NOX1 protein was examined by Western blot analysis in the aorta of control, AngII- and HFD-, and AngII-, HFD- and donepezil-treated ApoE-KO mice. The blot was scanned and the band density was quantified. Data are expressed as mean ± S.E.M. $^{*}P < 0.05$ vs control, $^{\#}P < 0.05$ vs HFD and AngII group. $n = 4$.

double-blind trial that examined the effect of tiotropium, one of the anticholinergics, in patients with COPD showed opposite results [22]. Treatment with tiotropium showed an insignificant decrease in the number of death in patients with COPD and significantly decreased the incidence of myocardial infarction compared with placebo. Therefore, the issue regarding the effect of anticholinergics treatment on cardiovascular events, in particular myocardial infarction, is still controversial.

Vascular oxidative stress accelerates atherosclerosis [23]. AngII induces ROS production via activation of NADPH oxidase. Subunits of NADPH oxidase such as p47phox, p22phox, and NOX play critical role in AngII induced ROS production because knockdown of these subunit inhibited ROS production by AngII and less vascular lesion was induced in mice lacking these subunit [19]. The reduction of mRNA expression of each NADPH oxidase subunits (p47phox, p22phox and NOX1) in donepezil-treated mice was not statistically significant. However, the expression of p47phox at the protein level was significantly reduced by donepezil. Although the mechanism for the difference between mRNA and protein level of p47phox is not clear, suppression of p47phox may explain the anti-oxidative effect of donepezil.

Donepezil suppressed aortic MCP-1 expression in ApoE-KO mice received HFD and AngII-infusion. MCP-1 is well known to enhance atherogenesis. However, MCP-1 deficiency did not affect atherosclerotic lesion size in LDL receptor knockout mice fed a normal chow but decreased lesion size those fed a western diet [24]. The lack of the effect of MCP-1 deficiency is explained by upregulation of MCP-5, which is highly homologous to MCP-1. This study suggests that single inhibition of MCP-1 is not sufficient to suppress atherogenesis due to activation of alternative pathways. In this regard, simultaneous suppression of TNF-α by donepezil might synergistically attenuate atherogenesis in ApoE-KO mice. A recent study showed that expression of hepatic MCP-1 mRNA was correlated with the degree of liver steatosis in LDL receptor knockout mice fed a HFD [25]. Therefore, it is interesting to address in the future whether donepezil ameliorates liver steatosis in ApoE-KO mice treated with a HFD and AngII-infusion.

Acetylcholine, a major neurotransmitter of vagus nerve, is known to activate endothelial nitric oxide (NO) synthase and dilate blood vessel [26]. However, acetylcholine is rapidly degraded by cholinesterase in a few seconds. Therefore, it may be possible that donepezil and physostigmine inhibition of cholinesterase increases the availability of acetylcholine and increases NO production. However, we could not see upregulation or phosphorylation of eNOS in the aorta of ApoE-KO mice treated with donepezil (data not shown). These data suggest that an increase in NO level may not be the major mechanism for the anti-atherosclerotic effect of donepezil.

At this point, the source of acetylcholine is not clear. Amenta et al. showed that cholinergic innervation of the aorta [27]. A nerve plexus in the adventitial layer has been identified in the mouse, suggesting that acetylcholine is derived from the nerve ending of the vagus. In contrast, recent studies suggest that macrophages and endothelial cells express choline acetyltransferase that produces acetylcholine from choline and acetyl-CoA [28]. Therefore, further study is needed to determine whether acetylcholine is derived from vagus nerve ending or locally produced from macrophages or endothelial cells.

The limitation of the present study is that we do not have a direct evidence that donepezil inhibited atherogenesis through an inhibition of cholinesterase. Because the dose of donepezil used in this study is very high, we could not exclude the possibility of a direct or non-specific anti-atherogenic effect of donepezil. However, physostigmine, another cholinesterase inhibitor structurally different from donepezil also suppressed atherogenesis in the same model, indicating that the anti-atherogenic effect is mediated by inhibition of cholinesterase but not by a direct or non-specific effect of the drug. Further study is needed to confirm this point.

Another limitation of the current study is that we used very high dose of donepezil compared with the dose clinically used for the treatment of Alzheimer's disease. Therefore, we must be cautious about extrapolating our results to human atherosclerosis. However, 5 mg/kg/day of donepezil is widely used to examine the effect on dementia in a rodent model [29] despite the clinical dose is 5–10 mg/day for Alzheimer's disease. Thus, differential susceptibility to the drug between human and mice, and a very short period for the development of the lesions in animal models may be the reason for the requirement for high doses to be effective.

In summary, we showed in the present study that treatment with donepezil attenuated atherogenesis in ApoE-KO mice possible through anti-oxidative and anti-inflammatory effects. Although we should be cautious in extrapolating current results to other atherosclerotic model or human atherosclerosis [30], cholinesterase inhibitors may be a novel strategy for the treatment of atherosclerotic cardiovascular diseases.

Acknowledgements

This study was supported in part by Grants-in-aid for Scientific Research from the Ministry of Education, Culture, Sports, Science and Technology of Japan (19590867), AstraZeneca Research grant 2007 (London, UK), Mitsubishi Pharma Research Foundation (Osaka, Japan), Astellas Foundation for Research on Metabolic Disorders (Tokyo, Japan) and Suzuken Memorial Foundation (Nagoya, Japan).

Appendix A. Supplementary data

Supplementary data associated with this article can be found, in the online version, at doi:10.1016/j.atherosclerosis.2010.07.027.

References

[1] Schwartz PJ, La Rovere MT. ATRAMI: a mark in the quest for the prognostic value of autonomic markers. Autonomic Tone and Reflexes After Myocardial Infarction. Eur Heart J 1998;19:1593–5.

[2] The Cardiac Insufficiency Bisoprolol Study II (CIBIS-II): a randomised trial. Lancet 1999;353:9–13.

[3] Li M, Zheng C, Sato T, et al. Vagal nerve stimulation markedly improves long-term survival after chronic heart failure in rats. Circulation 2004;109:120–4.

[4] Tsutsumi T, Ide T, Yamato M, et al. Modulation of the myocardial redox state by vagal nerve stimulation after experimental myocardial infarction. Cardiovasc Res 2008;77:713–21.

[5] Borovikova LV, Ivanova S, Zhang M, et al. Vagus nerve stimulation attenuates the systemic inflammatory response to endotoxin. Nature 2000;405:458–62.

[6] Wang H, Yu M, Ochani M, et al. Nicotinic acetylcholine receptor alpha7 subunit is an essential regulator of inflammation. Nature 2003;421:384–8.

[7] Wang H, Liao H, Ochani M, et al. Cholinergic agonists inhibit HMGB1 release and improve survival in experimental sepsis. Nat Med 2004;10:1216–21.

[8] de Jonge WJ, van der Zanden EP, The FO, et al. Stimulation of the vagus nerve attenuates macrophage activation by activating the Jak2-STAT3 signaling pathway. Nat Immunol 2005;6:844–51.

[9] Heeschen C, Jang JJ, Weis M, et al. Nicotine stimulates angiogenesis and promotes tumor growth and atherosclerosis. Nat Med 2001;7:833–9.

[10] Hansen RA, Gartlehner G, Webb AP, et al. Efficacy and safety of donepezil, galantamine, and rivastigmine for the treatment of Alzheimer's disease: a systematic review and meta-analysis. Clin Interv Aging 2008;3:211–25.

[11] Reale M, Iarlori C, Gambi F, et al. Acetylcholinesterase inhibitors effects on oncostatin-M, interleukin-1 beta and interleukin-6 release from lymphocytes of Alzheimer's disease patients. Exp Gerontol 2005;40:165–71.

[12] Dzau V. The cardiovascular continuum and renin–angiotensin–aldosterone system blockade. J Hypertens Suppl 2005;23:S9–17.

[13] Ni W, Kitamoto S, Ishibashi M, et al. Monocyte chemoattractant protein-1 is an essential inflammatory mediator in angiotensin II-induced progression of established atherosclerosis in hypercholesterolemic mice. Arterioscler Thromb Vasc Biol 2004;24:534–9.

[14] Garrido AM, Griendling KK. NADPH oxidases and angiotensin II receptor signaling. Mol Cell Endocrinol 2009;302:148–58.

[15] Handa T, Katare RG, Kakinuma Y, et al. Anti-Alzheimer's drug, donepezil, markedly improves long-term survival after chronic heart failure in mice. J Card Fail 2009;15:805–11.

[16] Bhat RV, Turner SL, Marks MJ, Collins AC. Selective changes in sensitivity to cholinergic agonists and receptor changes elicited by continuous physostigmine infusion. J Pharmacol Exp Ther 1990;255:187–96.

[17] Miller Jr FJ, Griendling KK. Functional evaluation of nonphagocytic NAD(P)H oxidases. Methods Enzymol 2002;353:220–33.

[18] Chun HJ, Ali ZA, Kojima Y, et al. Apelin signaling antagonizes Ang II effects in mouse models of atherosclerosis. J Clin Invest 2008;18:3343–54.

[19] Brandes RP, Schroder K. Composition and functions of vascular nicotinamide adenine dinucleotide phosphate oxidases. Trends Cardiovasc Med 2008;18:15–9.

[20] Custodis F, Baumhakel M, Schlimmer N, et al. Heart rate reduction by ivabradine reduces oxidative stress, improves endothelial function, and prevents atherosclerosis in apolipoprotein E-deficient mice. Circulation 2008;117:2377–87.

[21] Singh S, Loke YK, Furberg CD. Inhaled anticholinergics and risk of major adverse cardiovascular events in patients with chronic obstructive pulmonary disease: a systematic review and meta-analysis. JAMA 2008;300:1439–50.

[22] Tashkin DP, Celli B, Senn S, et al. 4-Year trial of tiotropium in chronic obstructive pulmonary disease. N Engl J Med 2008;359:1543–54.

[23] Cai H, Harrison DG. Endothelial dysfunction in cardiovascular diseases: the role of oxidant stress. Circ Res 2000;87:840–4.

[24] Rull A, Beltrán-Debón R, Aragonès G, et al. Expression of cytokine genes in the aorta is altered by the deficiency in MCP-1: effect of a high-fat, high-cholesterol diet. Cytokine 2010;50:121–8.

[25] Rull A, Rodríguez F, Aragonès G, et al. Hepatic monocyte chemoattractant protein-1 is upregulated by dietary cholesterol and contributes to liver steatosis. Cytokine 2009;48:273–9.

[26] Pepine CJ. The impact of nitric oxide in cardiovascular medicine: untapped potential utility. Am J Med 2009;122:S10–5.

[27] Amenta F, Cavallotti C, Ferrante F, Zomparelli M. The cholinergic innervation of the aorta. Acta Histochem 1980;66:197–203.

[28] Wessler I, Kirkpatrick CJ, Racke K. The cholinergic 'pitfall': acetylcholine, a universal cell molecule in biological systems, including humans. Clin Exp Pharmacol Physiol 1999;26:198–205.

[29] Saxena G, Singh SP, Agrawal R, Nath C. Effect of donepezil and tacrine on oxidative stress in intracerebral streptozotocin-induced model of dementia in mice. Eur J Pharmacol 2008;581:283–9.

[30] Joven J, Rull A, Ferré N, et al. The results in rodent models of atherosclerosis are not interchangeable: the influence of diet and strain. Atherosclerosis 2007;195(2):e85–92.

Blockade of mineralocorticoid receptors improves salt-induced left-ventricular systolic dysfunction through attenuation of enhanced sympathetic drive in mice with pressure overload

Koji Ito, Yoshitaka Hirooka and Kenji Sunagawa

Objectives In a pressure overload model, sympathetic activity is augmented in response to salt intake. Mineralocorticoid receptors and epithelial Na channels (ENaCs) are thought to contribute to Na-processing, but the underlying mechanism is unknown. Here, we investigated the contribution of the brain mineralocorticoid receptor–ENaC pathway to salt-induced sympathetic activation in a pressure overload model.

Methods and results Aortic banding was performed to produce a mouse pressure overload model. Four weeks after aortic banding (AB-4), left-ventricular (LV) wall thickness was increased without a change in percentage fractional shortening (%FS). Sympathetic activity increased in response to a 5-day high-salt diet in AB-4, but not in Sham-4. Brain mineralocorticoid receptor, αENaC, and angiotensin II type 1 receptor (AT1R) expression levels were greater in AB-4 than in Sham-4. The increase in sympathetic activity and in the expression of these proteins was blocked by intracerebroventricular (ICV) infusion of eplerenone, a mineralocorticoid receptor blocker. In another protocol, AB-4 mice were fed a high-salt diet (AB-H) for 4 additional weeks. At 4 weeks, %FS was decreased and sympathetic activity was increased in AB-H compared with Sham. Expression of mineralocorticoid receptors and AT1R in the brain was higher in AB-H than in Sham. ICV infusion of eplerenone in AB-H attenuated salt-induced sympathoexcitation and the decreased %FS. ICV infusion of eplerenone also decreased brain AT1R expression.

Conclusions These findings indicate that activation of brain αENaC and AT1R through mineralocorticoid receptors contributes to the acquisition of Na sensitivity to induce sympathoexcitation. Therefore, high salt intake accelerates sympathetic activation and LV systolic dysfunction in a pressure overload model. *J Hypertens* 28:1449–1458 © 2010 Wolters Kluwer Health | Lippincott Williams & Wilkins.

Journal of Hypertension 2010, 28:1449–1458

Keywords: brain, heart failure, pressure overload, salt, sympathetic nervous system

Abbreviations: %FS, percent fractional shortening; AB-4, AB mice 4 weeks postoperative; AB-H, AB mice fed a high salt diet; AB-R, AB mice fed a regular salt diet; AT1R, angiotensin II type 1 receptor; CSF, cerebrospinal fluid; ENaCs, epithelial Na channels; GAPDH, glyceraldehyde 3-phosphate dehydrogenase; ICV, intracerebroventricular; IgG, immunoglobulin; LV, left ventricle; LVDD, LV end-diastolic diameter; LVSD, LV end-systolic diameter; LVWT, LV wall thickness; Sham, sham-operated mice; Sham-4, Sham mice 4 weeks postoperative; Sham-H, Sham mice fed a high salt diet; Sham-R, Sham mice fed a regular salt diet; U-NE, 24-h urinary norepinephrine

Department of Cardiovascular Medicine, Kyushu University Graduate School of Medical Sciences, Fukuoka, Japan

Correspondence to Yoshitaka Hirooka, MD, PhD, FAHA, Department of Cardiovascular Medicine, Kyushu University Graduate School of Medical Sciences, 3-1-1, Higashi-ku, Fukuoka 812-8582, Japan
Tel: +81 92 642-5360; fax: +81 92 642 5374;
e-mail: hyoshi@cardiol.med.kyushu-u.ac.jp

Received 8 September 2009 **Revised** 22 December 2009
Accepted 15 February 2010

Introduction

High salt intake induces hypertension in a salt-sensitive hypertensive animal model via sympathetic nerve activation [1,2]. The central nervous system plays an important role in salt-induced hypertension. An increase in Na in the cerebrospinal fluid (CSF) is an important step in salt-induced hypertension. High salt intake increases CSF Na only in salt-sensitive hypertensive rats, however, and not in salt-resistant normotensive rats [3]. Intracerebroventricular (ICV) infusion of high-Na containing CSF causes hypertension in both salt-sensitive hypertensive rats and salt-resistant normotensive rats via brain angiotensin type 1 receptor (AT1R) activation [4]. Enhanced Na uptake from the plasma to the CSF might therefore be an important step in the initiation of salt-induced hypertension in salt-sensitive hypertensive rats. Epithelial Na channels (ENaCs) on the blood side of the choroidal epithelium contribute to Na transport in the CSF [5,6]. In addition, ENaCs are activated through the activation of mineralocorticoid receptors [7,8]. Thus, the mineralocorticoid receptor–ENaC pathway might be involved in the enhanced Na uptake into the CSF in the salt-sensitive hypertensive model.

We recently reported that mice with pressure overload become sensitive to physiologic brain levels of Na, thereby acquiring a lower threshold for sympathetic activation [9]. Whether the brain mineralocorticoid receptor–ENaC pathway is involved in the salt-sensitive sympathetic activation in mice with pressure overload, however, is not clear. Therefore, the aim of the present study was to examine the expression levels of brain mineralocorticoid receptors and ENaCs in mice with pressure overload, and to determine whether mineralocorticoid receptor

0263-6352 © 2010 Wolters Kluwer Health | Lippincott Williams & Wilkins DOI:10.1097/HJH.0b013e328338bb37

Fig. 1

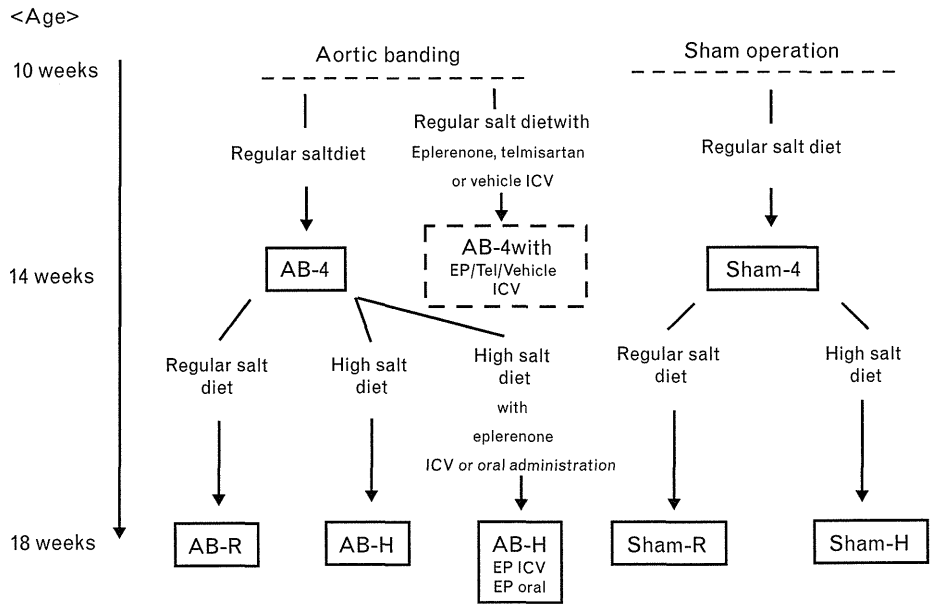

Experimental protocol and time-line. W indicates weeks; ICV, intracerebroventricular.

antagonism attenuates salt-induced sympathetic activation and improves left-ventricular (LV) systolic function in mice with pressure overload. Toward this aim, we investigated the expression of brain mineralocorticoid receptor and ENaCs in mice with pressure overload; the sympathetic activity in response to a 5-day high-salt diet in mice with pressure overload to confirm the acquisition of Na sensitivity; the effects of ICV infusion or oral administration of eplerenone, a selective mineralocorticoid receptor blocker [10,11], concomitant with high-salt loading on sympathetic activity and LV systolic function in mice with pressure overload.

Methods

Animals

The study was reviewed and approved by the Committee on Ethics of Animal Experiments, Kyushu University Graduate School of Medical Sciences, and conducted according to the Guidelines for Animal Experiments of Kyushu University. Male Institute of Cancer Research (ICR) mice (10 weeks old; SLC, Fukuoka, Japan) were used.

Mouse pressure overload model preparation

The suprarenal abdominal aorta [9,12] was banded in mice (AB mice) under sodium pentobarbital (25–40 mg/kg i.p.) anesthesia. The abdominal aorta was constricted at the suprarenal level with 5-0 silk sutures guided by a blunted 27-gauge needle, which was withdrawn as quickly as possible. Sham-operated (Sham) mice served as controls. Four weeks later, mice (AB-4 mice or Sham-4 mice) were each divided randomly into two groups: mice fed a high-salt (8% NaCl) diet for 4 weeks (AB-H mice and Sham-H mice) and mice fed a regular-salt (0.3% NaCl) diet for 4 weeks (AB-R mice and Sham-R mice; Fig. 1).

Evaluation of left-ventricular systolic function

Left-ventricular systolic function was evaluated by echocardiography [9,13,14]. Serial M-mode echocardiography was performed on mice under light sodium pentobarbital anesthesia with spontaneous respiration. We used an echocardiography system (SSD5000; Aloka, Tokyo, Japan) with a dynamically focused 7.5-MHz linear array transducer. M-mode tracings were recorded from the short-axis view at the level of the papillary muscle. Left ventricle end-diastolic diameter (LVDD), LV end-systolic diameter (LVSD), and LV wall thickness (LVWT) were measured. LVWT was calculated as the mean thickness of the interventricular septum and the posterior LV wall. Percentage fractional shortening (%FS) was calculated as follows: $\%FS = (LVDD - LVSD)/LVDD \times 100$.

Evaluation of sympathetic activity

Sympathetic activity was evaluated by measuring 24-h urinary norepinephrine (U-NE) excretion using high-performance liquid chromatography [9,13,14].

Confirmation of acquired Na sensitivity in AB-4 mice

Sympathetic activity in response to a 5-day high-salt diet was evaluated as follows: both AB-4 mice and Sham-4

mice were fed a high-salt diet (8%) or a regular-salt diet for 5 days, and then U-NE was measured. Sympathetic activity in response to the high salt intake was evaluated in each group. In addition, ICV infusion of high-Na (0.2 mol/l) or regular-Na (0.145 mol/l) CSF (infusion rate: 0.25 μl/h for 5 days) was performed using an osmotic minipump, as follows. Under sodium pentobarbital anesthesia (25–40 mg/kg i.p.), mice were placed in a stereotaxic frame. The skin overlying the midline of the skull was incised, and a small hole was made with a dental drill at the following coordinates: 0.3 mm posterior and 1 mm lateral relative to bregma. The infusion cannula from an Alzet brain infusion kit 3 (DURECT Corporation, CA) connected to an osmotic minipump (Alzet model 1004; DURECT) was lowered 3 mm from the skull surface and fixed to the skull surface with tissue adhesive. The osmotic minipump was inserted subcutaneously in the back [9].

Measurement of organ weight

After completion of the experiments, the mice were killed with an overdose of sodium pentobarbital, and the heart and lungs were removed and weighed.

Measurement of blood pressure and heart rate

Under sodium pentobarbital anesthesia (25–40 mg/kg i.p.), mice were intubated using a 20-gauge soft catheter and ventilated with a tidal volume of 1.0–1.5 ml at 120 cycles/min with the fraction of inspired oxygen equal to 0.21 [9,13,14]. A catheter was then inserted into the right carotid artery to measure blood pressure and heart rate.

Treatment with eplerenone, a mineralocorticoid receptor blocker

To evaluate the effects of brain mineralocorticoid receptor antagonism on sympathetic activity in response to the high-salt diet in AB-4 mice, ICV infusion of the specific mineralocorticoid receptor blocker eplerenone [10,11] (0.3 mg/ml in CSF, infusion rate at 0.11 μl/h, kindly provided by Pfizer Pharmaceutical Company Inc., New York, New York, USA) was started concomitant with the aortic banding procedure and continued for 4 weeks. ICV infusion was performed as described above.

In another protocol, to evaluate the effects of brain mineralocorticoid receptor antagonism on salt-induced sympathetic activation and LV systolic dysfunction, eplerenone was administered by ICV infusion (0.3 mg/ml in CSF, infusion rate at 0.11 μl/h) or oral administration (100 mg/kg per day) for 4 weeks, concomitant with high-salt loading (AB-H mice). U-NE excretion, organ weight, blood pressure, and heart rate were measured, and echocardiography was performed as described above.

Evaluation of brain mineralocorticoid receptor, epithelial Na channels, and AT1R expression

The animals were killed with an overdose of sodium pentobarbital, and the circumventricular tissues including the hypothalamus were obtained. The tissues were homogenized in a lysing buffer containing 40 mmol/l HEPES [4-(2-hydroxyethyl)-1-piperazineethanesulfonic acid], 1% Triton X-100, 10% glycerol, 1 mmol/l sodium orthovanadate, and 1 mmol/l phenylmethylsulfonyl fluoride. Protein concentration was determined using a bicinchoninic acid protein assay kit (Pierce Chemical Co., Rockford, Illinois, USA). A 15-μg aliquot of protein from each sample was separated on a polyacrylamide gel with 10% sodium dodecyl sulfate. The proteins were subsequently transferred onto polyvinylidene difluoride membranes (Immobilon-P membranes; Millipore, Billerica, Massachusetts, USA). Membranes were incubated with rabbit immunoglobulin G (IgG) polyclonal antibody to mineralocorticoid receptors (1 : 1000; Santa Cruz Biotechnology, Santa Cruz, California, USA), with goat IgG polyclonal antibody to αENaC, rabbit polyclonal antibody to βENaC, rabbit polyclonal antibody to γENaC (1 : 1000, Santa Cruz Biotechnology), or with rabbit IgG monoclonal antibody to AT1R (1 : 1000, Santa Cruz Biotechnology). Membranes were then incubated with horseradish peroxidase-conjugated horse antirabbit or antigoat IgG antibody (1 : 10 000). Glyceraldehyde 3-phosphate dehydrogenase (GAPDH) was used as an internal control for the brain tissues. Immunoreactivity was detected by enhanced chemiluminescence autoradiography (ECL Western blotting detection kit; Amersham Pharmacia Biotech, Uppsala, Sweden), and the film was analyzed using the public domain software NIH Image (developed at the US National Institutes of Health and available on the Internet at http://rsb.info.nih.gov/nih-image/).

Evaluation of effects of eplerenone on brain epithelial Na channels and AT1R expression

To evaluate the effects of brain mineralocorticoid receptor antagonism on AT1R and ENaCs, we performed western blot analysis for AT1R, αENaC, and γENaC in the circumventricular tissues including the hypothalamus of AB-4 mice (AT1R and αENaC) or AB-H mice(AT1R and γENaC) with or without ICV infusion of eplerenone. ICV infusion of eplerenone and western blot analysis were performed as described above.

Evaluation of the effects of telmisartan, an AT1R blocker, on brain mineralocorticoid receptor and αENaC expression

To evaluate the effects of brain AT1R blockade on brain mineralocorticoid receptor and αENaC expression in AB-4 mice, we performed western blot analysis of mineralocorticoid receptor and αENaC in the circumventricular tissues, including the hypothalamus, of AB-4 mice with or without ICV infusion of telmisartan. ICV infusion of the AT1R blocker telmisartan [4 mmol/l in dimethyl sulfoxide (DMSO, Sigma Chemical Co) infusion rate at 0.11 μl/h for 28 days] [9] and western blot analysis were performed as described above.

Fig. 2

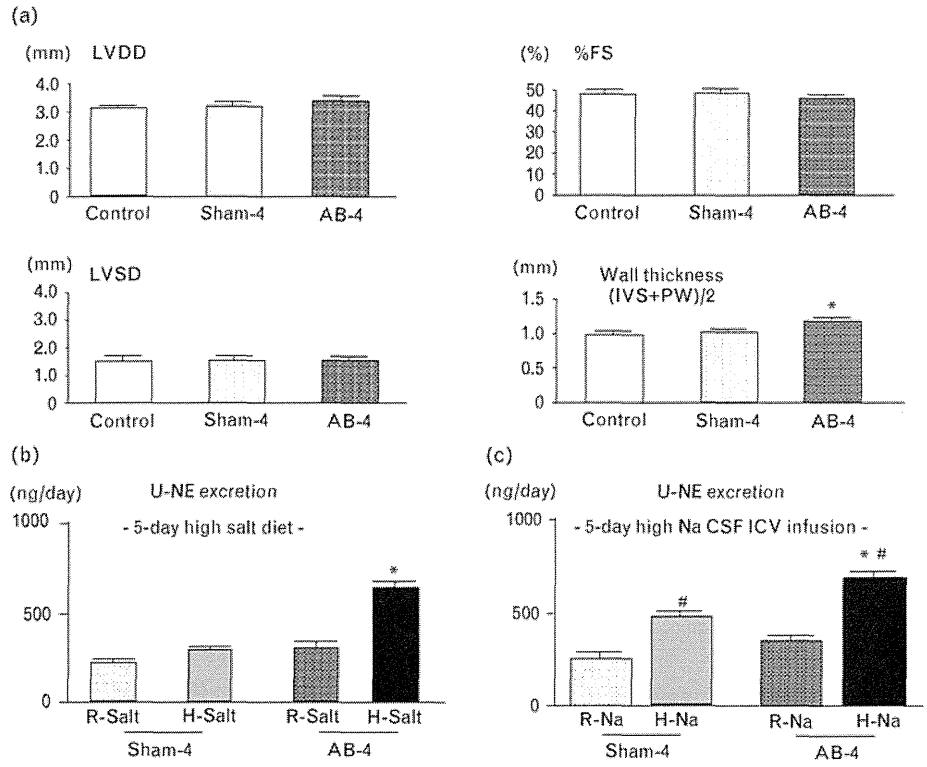

(a) Cardiac function in each group. %FS, percentage fractional shortening; IVS, interventricular septum; LVDD, left-ventricular end-diastolic diameter; LVSD, left-ventricular systolic diameter; PW, posterior wall. $^{*}P < 0.05$ versus other group, $n = 5$ for each. (b) U-NE excretion in response to 5-day high-salt diet in each group. H-salt, high-salt diet; R-salt, regular-salt diet. $^{*}P < 0.05$ versus R-salt, $n = 7-8$. (c) U-NE excretion in response to 5-day ICV infusion of high-Na CSF in each group. H-Na, high-Na CSF; R-Na, regular-Na CSF. $^{\#}P < 0.05$ versus R-Na, $^{*}P < 0.05$ versus Sham-4 H-Na, $n = 7$ for each. CSF, cerebrospinal fluid; ICV, intracerebroventricular; U-NE, urinary norepinephrine.

Statistical analysis

All values are expressed as mean ± SE. Analysis of variance was used to compare U-NE, organ weight, LVDD, LVSD, LVWT, %FS, and protein expression levels between groups. An unpaired *t*-test was used to compare changes in protein levels between AB-H mice treated with and without eplerenone. Differences were considered to be significant when the *P* value was less than 0.05.

Results

Characteristics of AB-4 mice

Neither relative heart weight (heart weight/body weight) nor absolute heart weight differed between AB-4 mice and Sham-4 mice (relative heart weight: Sham-4, 5.08 ± 0.11; AB-4, 5.10 ± 0.10, absolute heart weight: Sham-4, 0.23 ± 0.04 g; AB-4, 0.23 ± 0.06 g, $n = 4$ for each). Relative lung weight (lung weight/body weight) also did not differ between groups (relative lung weight: Sham-4, 5.64 ± 0.21 g; AB-4, 5.90 ± 0.23 g, $n = 4$ for each).

Echocardiography revealed the following characteristics (Fig. 2a): LVWT was greater in AB-4 mice than in Sham-4 mice. The LV dimension and %FS, however, did not differ between groups.

Sympathetic activity evaluated by U-NE excretion in response to the 5-day high-salt diet was increased in AB-4 mice, but not in Sham-4 mice (Fig. 2b). Sympathetic activity in response to a 5-day ICV infusion of high-Na CSF was increased in both Sham-4 mice and AB-4 mice (Fig. 2c). LV systolic function evaluated by echocardiography did not change after the 5-day high-salt diet or after 5-day ICV infusion of high-Na CSF in either AB-4 mice or Sham-4 mice (data not shown).

Mineralocorticoid receptor, epithelial Na channel, and AT1R expression in the circumventricular tissue in AB-4 mice

Mineralocorticoid receptor expression was significantly greater in AB-4 mice than in Sham-4 mice (Fig. 3a). αENaC expression was significantly increased in AB-4 mice compared with Sham-4 mice (Fig. 3b), but βENaC and γENaC expression did not differ between groups (Fig. 3c). AT1R expression was greater in AB-4 mice than in Sham-4 mice (Fig. 3d). The enhanced brain αENaC and AT1R expression was attenuated by ICV infusion of eplerenone (Fig. 3b,d). The enhanced brain mineralocorticoid receptor and αENaC expressions did not

Fig. 3

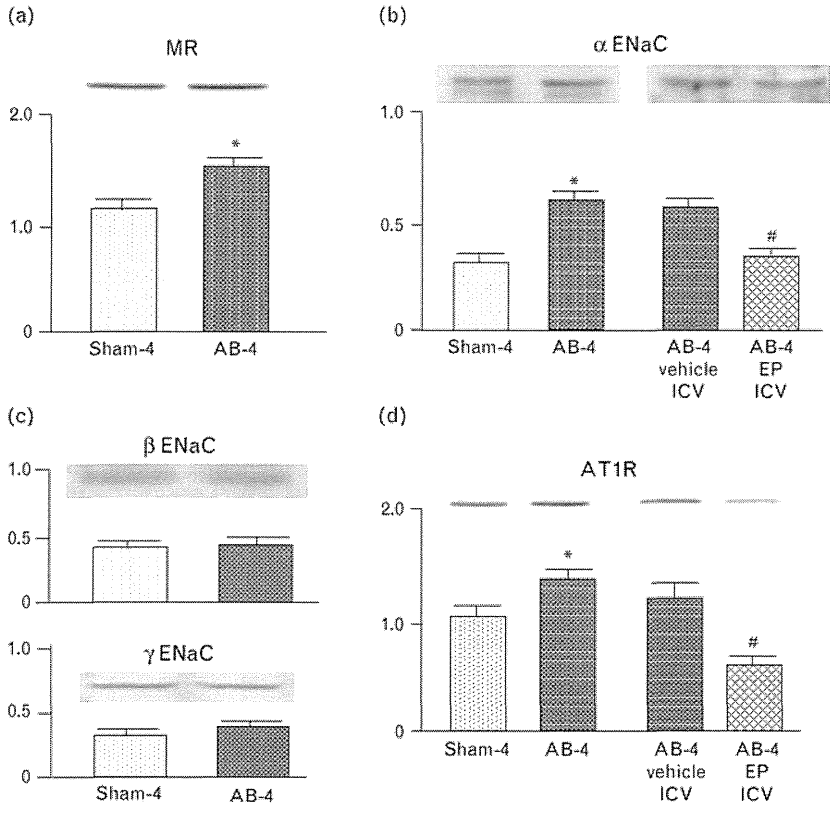

(a–c)Representative western blots showing MR, α, β, and γENaC expression in the brain from each group of mice. The graph shows the means for the quantification of four separate experiments. Data are expressed as the relative ratio to GAPDH expression. $^{*}P<0.05$ versus Sham-4, $^{\#}P<0.05$ versus AB-4 vehicle ICV. (d) Representative western blots showing AT1R expression in the brain. The graphs show the means for the quantification of three separate experiments. Data are expressed as the relative ratio to GAPDH expression. $^{*}P<0.05$ versus Sham-4, $^{\#}P<0.05$ versus AB-4 vehicle ICV. AT1R, angiotensin II type 1 receptor; EP, eplerenone; GAPDH, glyceraldehyde 3-phosphate dehydrogenase; ICV, intracerebroventricular infusion; MR, mineralocorticoid receptor.

change by ICV infusion of telmisartan (relative abundance of mineralocorticoid receptor/GAPDH: 1.76 ± 0.12 in AB-4 with vehicle versus 1.67 ± 0.11 in AB-4 with telmisartan, relative abundance of αENaC/GAPDH: 0.59 ± 0.08 in AB-4 with vehicle versus 0.61 ± 0.09 in AB-4 with telmisartan $n=3$ for each).

Effects of eplerenone on sympathetic activity in response to high-salt diet

Intracerebroventricular infusion of eplerenone started concomitantly with aortic banding attenuated sympathetic activity in response to the 5-day high-salt diet in AB-4 mice (U-NE: AB-4 high-salt diet with eplerenone, 397 ± 40 ng/day; AB-4 high-salt diet without eplerenone, 650 ± 30 ng/day, $n=5$–7).

Effects of long-term high-salt intake on sympathetic activity and left-ventricular systolic function in AB-H mice

Relative heart weight (heart weight/body weight) was significantly increased in AB-H mice compared with Sham mice (Sham-R, 4.81 ± 0.10; Sham-H, 5.11 ± 0.18; AB-R, 5.54 ± 0.20; AB-H, 6.62 ± 0.21, $n=4$ for each). Absolute heart weight was also significantly greater in AB-H mice than in Sham mice (Sham-R, 0.23 ± 0.01 g; Sham-H, 0.24 ± 0.02 g; AB-R, 0.25 ± 0.01 g; AB-H, 0.27 ± 0.02 g, $n=4$ for each). Relative lung weight (lung weight/body weight) did not differ significantly between groups (Sham-R, 5.81 ± 0.21; Sham-H, 5.73 ± 0.14; AB-R, 5.94 ± 0.12; AB-H, 6.24 ± 0.23, $n=4$ for each). Body weight was significantly lower in AB mice than in Sham mice (Sham-R, 47.8 ± 0.5 g; Sham-H, 47.1 ± 0.5; AB-R, 44.2 ± 0.9; AB-H, 40.2 ± 0.4, $n=4$ for each).

Echocardiography revealed the following characteristics (Fig. 4a): LVWT was greater in AB mice than in Sham mice. %FS was significantly lower in AB-R mice than in Sham mice and further decreased in AB-H mice than in AB-R mice. The LV size was significantly higher in AB-H mice than in the other groups. Echocardiography revealed no significant differences between Sham-R mice and Sham-H mice.

Sympathetic activity evaluated by U-NE excretion was significantly higher in AB-H mice than in the other

Fig. 4

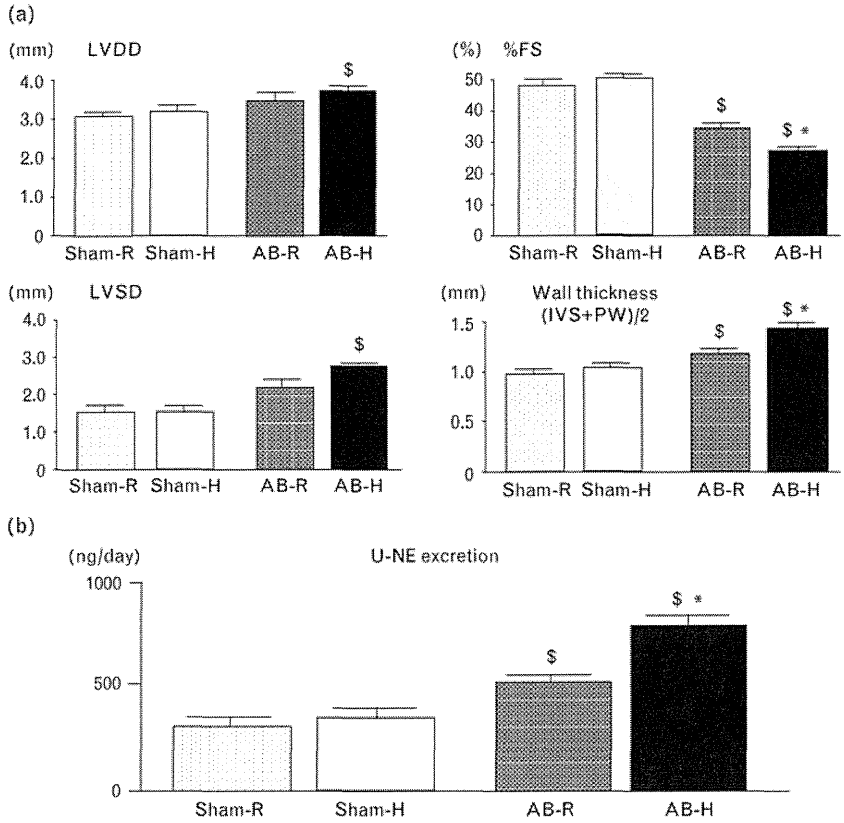

(a) Cardiac function in each group. %FS, percentage fractional shortening; IVS, interventricular septum; LVDD, left-ventricular end-diastolic diameter; LVSD, left-ventricular systolic diameter; PW, posterior wall. $^{\$}P < 0.05$ versus Sham mice (Sham-R and Sham-H), $^{*}P < 0.05$ versus AB-R, $n = 5$ for each. (b) Sympathetic activity evaluated by U-NE excretion in each group. $\$P < 0.05$ versus Sham mice (Sham-R and Sham-H), $^{*}P < 0.05$ versus AB-R, $n = 10$ for each. U-NE, urinary norepinephrine.

groups (Fig. 4b). Blood pressure in AB-H mice tended to be lower, and heart rate was significantly higher than that in the other groups [mean blood pressure (mmHg): 99 ± 5 in Sham-R, 95 ± 2 in Sham-H, 90 ± 3 in AB-R, 82 ± 2 in AB-H, heart rate (b.p.m.): 409 ± 7 in Sham-R, 428 ± 5 in Sham-H, 440 ± 6 in AB-R, 464 ± 8 in AB-H, $n = 5$ for each].

Mineralocorticoid receptor, epithelial Na channel, and AT1R expression in the circumventricular tissue in AB-H mice

Mineralocorticoid receptor expression was significantly greater in AB-H mice than in Sham mice (Fig. 5a). Mineralocorticoid receptor expression in AB-R mice was similar to that in AB-H mice. Mineralocorticoid receptor expression in Sham-H mice did not differ from that in Sham-R mice.

αENaC expression did not differ between groups (Sham-R, Sham-H, AB-R, and AB-H mice; Fig. 5b). γENaC expression, however, was significantly increased in AB-H mice compared with Sham mice. γENaC expression in AB-R mice was similar to that in AB-H mice. γENaC expression in Sham-H mice did not differ from that in Sham-R mice. ICV infusion of eplerenone (administered concomitantly with a high-salt diet) did not attenuate the enhanced γENaC expression (Fig. 5c). βENaC expression did not differ between groups (Fig. 5b). AT1R expression in AB-H was significantly greater than in Sham mice, and ICV infusion of eplerenone attenuated this increase (Fig. 5d).

Effects of eplerenone on left-ventricular systolic function and sympathetic activity in AB-H mice

Intracerebroventricular infusion of eplerenone significantly decreased both relative and absolute heart weight and significantly improved LV systolic function (decreased LVDD and LVSD, increased %FS) in AB-H mice (Fig. 6a). Sympathetic activity was also decreased by ICV infusion of eplerenone in AB-H mice (Fig. 6b). The effects of oral administration of eplerenone were similar to those of ICV infusion. Oral administration of eplerenone had smaller effects on U-NE excretion and %FS than ICV infusion, although oral administration had

Fig. 5

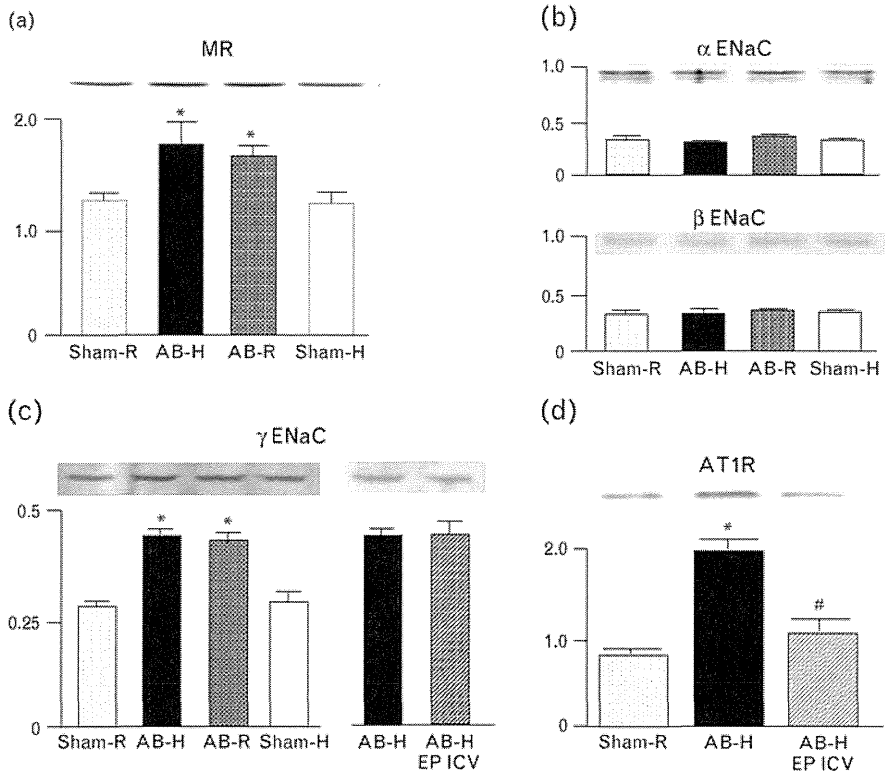

(a) Representative western blots showing MR expression in the brain from each group of mice. The graph shows the means for the quantification of five separate experiments. Data are expressed as the relative ratio to GAPDH expression. $^{*}P < 0.05$ versus Sham mice (Sham-R and Sham-H). (b-c) Representative western blots showing α, β, and γENaC expression in the brain from each group of mice. The graph shows the means for the quantification of three separate experiments. Data are expressed as the relative ratio to GAPDH expression. $^{*}P < 0.05$ versus Sham mice (Sham-R and Sham-H). (d) Representative western blots showing AT1R expression in the brainfrom each group of mice. The graph shows the means for the quantification of three separate experiments. Data are expressed as the relative ratio to GAPDH expression. $^{*}P < 0.05$ versus Sham-R, $^{\#}P < 0.05$ versus AB-H. AT1R, angiotensin II type 1 receptor; EP, eplerenone; GAPDH, glyceraldehyde 3-phosphate dehydrogenase; ICV, intracerebroventricular infusion; MR, mineralocorticoid receptor.

greater effects on LV hypertrophy than ICV infusion (Fig. 6a,b). Neither ICV infusion nor oral administration of eplerenone altered blood pressure [mean blood pressure (mmHg): 82 ± 2 in AB-H versus 88 ± 2 in AB-H with ICV eplerenone, 86 ± 1 in AB-H with oral eplerenone, $n = 5$ for each]. Heart rate, however, was significantly lower in mice treated with either ICV infusion or oral administration of eplerenone [heart rate (b.p.m.): 464 ± 8 in AB-H versus 430 ± 6 in AB-H with ICV eplerenone, 436 ± 12 in AB-H with oral eplerenone, $n = 5$ for each].

Discussion

The present study demonstrated the following: 4 weeks after aortic banding, mice had LV hypertrophy without a decrease in %FS (AB-4 mice); sympathetic activity in response to high salt intake was augmented in AB-4 mice via brain mineralocorticoid receptor-modulated αENaC and AT1R activation; and both ICV infusion and oral administration of eplerenone, a selective mineralocorticoid receptor blocker, attenuated salt-induced sympathetic activation and improved LV systolic function in AB-H mice. These findings indicate that mineralocorticoid receptor antagonism may be a useful strategy to prevent sympathetic activation in response to high salt intake in patients with pressure overload, such as hypertensive heart disease. Furthermore, these effects of mineralocorticoid receptor antagonism may improve LV systolic function by attenuating salt-induced sympathetic activation.

The enhanced brain mineralocorticoid receptor, αENaC, and AT1R expression in AB-4 mice is an important finding in the present study. Brain mineralocorticoid receptor, ENaCs, and AT1R are involved in sympathetic activation in a salt-sensitive hypertensive model [15], a model of high-Na CSF induced hypertension [4], and a myocardial infarction model [16]. Using a mineralocorticoid receptor antagonist in the present study, we confirmed these previous observations. These previous studies, however, did not evaluate whether the expression of these proteins was increased. Therefore, we investigated brain mineralocorticoid receptor, ENaC, and AT1R expression and

Fig. 6

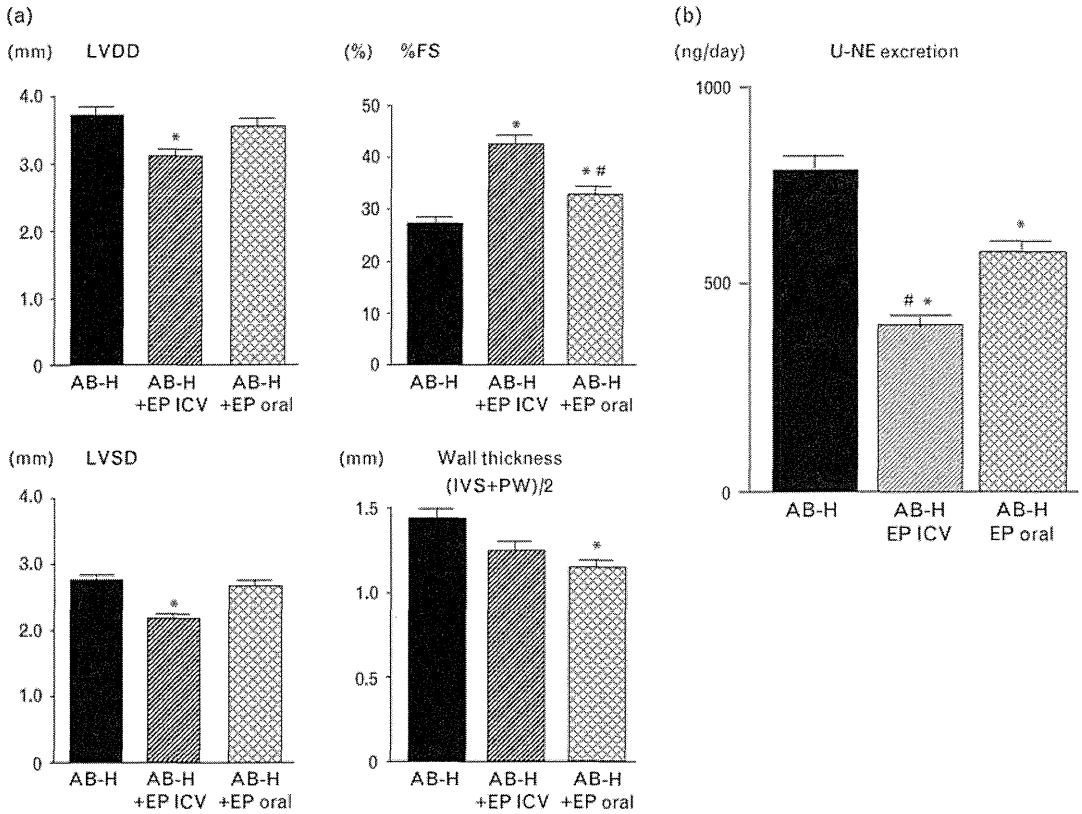

(a) Cardiac function in each group. EP, eplerenone; %FS, percentage fractional shortening; ICV, intracerebroventricular infusion, IVS, interventricular septum; LVDD, left-ventricular end-diastolic diameter; LVSD, left-ventricular systolic diameter; PW, posterior wall. $^{*}P < 0.05$ versus AB-H, $^{\#}P < 0.05$ versus AB-H EP ICV, $n = 5$ each. (b) Sympathetic activity evaluated by U-NE excretion in each group. EP, eplerenone; ICV, intracerebroventricular infusion. $^{*}P < 0.05$ versus AB-H mice, $^{\#}P < 0.05$ versus AB-H EP ICV mice, $n = 6$ in AB-H EP ICV and EP oral, $n = 10$ in AB-H.

confirmed the enhanced expression of these proteins in AB-4 mice. Furthermore, we confirmed that ICV infusion of eplerenone attenuated the enhanced brain αENaC and AT1R expression, but ICV infusion of telmisartan failed to attenuate the enhanced expression of brain mineralocorticoid receptor and αENaC. These results strongly suggest that, in AB-4 mice, activation of the brain MR-αENaC pathway leads to AT1R activation. This brain mineralocorticoid receptor–αENaC pathway activation may facilitate Na uptake from plasma to the CSF, because ENaCs on the blood side of the choroidal epithelium have an important role in Na transport into the CSF [5,6]. Therefore, activation of the brain mineralocorticoid receptor–αENaC pathway is considered to be an initial step in the acquisition of Na sensitivity in the brain in a pressure overload model.

We confirmed the important role of the brain mineralocorticoid receptor–αENaC pathway in the acquisition of Na sensitivity in a pressure overload model. Sympathetic activity in response to the 5-day high-salt diet was increased in AB-4 mice, but not in Sham-4 mice. On the contrary, sympathetic activity in response to ICV infusion of high-Na CSF was increased in both Sham-4 mice and AB-4 mice. These results support the notion that enhanced Na uptake into the CSF is an important factor in salt-induced sympathetic activation in a pressure overload model. Furthermore, the 5-day high-salt diet-induced sympathetic activation in AB-4 mice was attenuated by ICV infusion of eplerenone started concomitantly with aortic banding. These results indicate that the brain mineralocorticoid receptor–αENaC pathway has an important role in the acquisition of Na sensitivity in the brain in a pressure overload model. Although U-NE was increased by ICV infusion of high-Na CSF in both AB-4 mice and Sham-4 mice, the extent of the increase was greater in AB-4 mice than in Sham-4 mice, suggesting that sensitivity to Na in the CSF was increased in AB-4 mice. These findings support those in our previous study [9], but the underlying mechanism remains unclear. In addition to the mineralocorticoid receptor-modulated increase in αENaC expression in the brain, in the present study we confirmed that mineralocorticoid receptor also modulates the expression of AT1R in the brain.

Therefore, enhanced AT1R expression might contribute to the increased responsiveness to Na in the CSF in AB-4 mice.

To clarify the effects of long-term high-salt diet on sympathetic activity and LV systolic function in a pressure overload model, we fed AB-4 mice and Sham-4 mice a high-salt or regular-salt diet for 4 weeks. U-NE excretion increased in AB-R mice compared with Sham mice, and further increased in AB-H mice compared with AB-R mice. LVWT increased and %FS decreased in AB-R mice compared with Sham mice, and both alterations were more severe in AB-H mice than in AB-R mice. U-NE excretion and LVWT, and %FS did not differ between Sham-H mice and Sham-R mice. Blood pressure was lower and heart rate was higher in AB-H mice than in the other groups, suggesting low cardiac output and sympathetic activation [9]. These results strongly suggest that, in a pressure-overload model, long-term high-salt intake accelerates sympathetic activation, resulting in the deterioration of LV systolic function.

Another important finding of the present study was that the enhanced brain mineralocorticoid receptor expression in the pressure-overload model was maintained in AB-H mice, and treatment with eplerenone reduced salt-induced sympathetic activation and LV systolic dysfunction in the AB-H mice. These results indicate that activation of the brain mineralocorticoid receptor pathway is sustained under high-salt loading in AB-H mice. Because serum aldosterone levels are significantly decreased in this model [9], activation of the brain mineralocorticoid receptor in AB-H mice might be independent of systemic aldosterone levels. CSF-Na may increase the local production of aldosterone in the brain [15,17], or there may be aldosterone-independent mineralocorticoid receptor activation [18]. The present study, however, did not address these issues, and further studies are needed to clarify the mechanisms of the enhanced expression of brain mineralocorticoid receptor in AB mice.

Both ICV infusion and oral administration of eplerenone for 4 weeks concomitantly with high-salt loading in AB-H mice attenuated the salt-induced sympathetic activation and improved LV systolic dysfunction. Because CSF eplerenone concentrations were not measured in the present study we cannot determine the concentration of eplerenone in the brain required to induce these observations via central mechanisms. In the present study, oral administration of eplerenone attenuated LV hypertrophy, which might be a direct effect of oral administration of eplerenone on the myocardium [10,11]. Blood pressure is another factor involved in LV hypertrophy. In the present study, neither oral administration nor ICV infusion of eplerenone affected blood pressure in AB-H mice. Blood pressure was measured under anesthesia, however, and we did not evaluate the 24-h blood pressure. Therefore, we cannot exclude the possibility that blood pressure affected LV hypertrophy. Heart rate was significantly decreased in AB-H with eplerenone, suggesting that sympathetic activity was attenuated. The dose of eplerenone was based on the maximum water solubility of eplerenone in an ICV infusion study, and by the most commonly used dose of eplerenone as a specific mineralocorticoid receptor blocker in oral administration studies [19,20,21]. In a previous study, eplerenone was injected into the hypothalamus at a dose of 0.13 mg/ml, 18 μl/h [22]. In the present study, we performed ICV infusion. In ICR mice, the CSF volume is approximately 36 μl [23]. Therefore, the dose of ICV-infused eplerenone in the present study was a relatively small dose (0.3 mg/ml, 0.11 μl/h) that should have produced an end concentration that acts as a specific mineralocorticoid receptor antagonist.

To explore the mechanisms of the inhibitory effects of eplerenone on salt-induced sympathetic activation and LV systolic dysfunction, we focused on the mineralocorticoid receptor–ENaC pathway. First, we examined the brain ENaC expression in both high-salt and regular-salt Sham mice and AB mice. Unlike in the AB-4 mice, the expression of αENaC did not differ between groups. The expression of γENaC, however, was significantly greater in AB-R mice than in Sham mice. Furthermore, this enhanced expression of γENaC was also evident in AB-H mice. Because of the enhanced brain γENaC expression in AB-H mice, we investigated the effects of ICV infusion of eplerenone on brain γENaC expression. The expression of γENaC was not decreased by ICV infusion of eplerenone. This finding suggests that the enhanced brain γENaC expression is independent of mineralocorticoid receptor activation. Therefore, we examined the involvement of the brain mineralocorticoid receptor–AT1R pathway in the salt-induced sympathetic activation in AB-H mice because we previously confirmed that ICV infusion of an AT1R blocker attenuated the salt-induced sympathetic activation in AB-H mice because we previously confirmed that ICV infusion of an AT1R blocker attenuated the salt-induced sympathetic activation in AB-H mice [9], and also mineralocorticoid receptor blockade attenuates the renin–angiotensin system [24]. The expression of AT1R in the brain was significantly higher in AB-H mice than in Sham mice, and this enhanced expression of AT1R was attenuated by ICV infusion of eplerenone. The brain renin–angiotensin system is activated in a heart failure model [25,26] and contributes to sympathetic hyperactivation [27,28]. These results suggest that the inhibitory effects of eplerenone on salt-induced sympathetic activation and LV systolic dysfunction result from the suppression of AT1R activity.

We evaluated three ENaC subunits, αENaC, βENaC, and γENaC [29]. We demonstrated mineralocorticoid receptor-dependent αENaC enhancement in AB-4 mice,